Suppression of colitis in mice by Cl-amidine: a novel peptidylarginine deiminase inhibitor.

Am J Physiol Gastrointest Liver Physiol 300: G929–G938, 2011.
First published March 17, 2011; doi:10.1152/ajpgi.00435.2010.

Suppression of colitis in mice by Cl-amidine: a novel peptidylarginine deiminase inhibitor

Alexander A. Chumanevich,[1] Corey P. Causey,[2] Bryan A. Knuckley,[2,3] Justin E. Jones,[2,3] Deepak Poudyal,[1] Alena P. Chumanevich,[1] Tia Davis,[4] Lydia E. Matesic,[4] Paul R. Thompson,[2,3] and Lorne J. Hofseth[1]

[1]*Department of Pharmaceutical and Biomedical Sciences, South Carolina College of Pharmacy, Departments of* [2]*Chemistry and Biochemistry and* [4]*Biological Sciences, University of South Carolina, Columbia, South Carolina; and* [3]*Department of Chemistry, The Scripps Research Institute, Scripps Florida, Jupiter, Florida*

Submitted 27 September 2010; accepted in final form 11 March 2011

Chumanevich AA, Causey CP, Knuckley BA, Jones JE, Poudyal D, Chumanevich AP, Davis T, Matesic LE, Thompson PR, Hofseth LJ. Suppression of colitis in mice by Cl-amidine: a novel peptidylarginine deiminase inhibitor. *Am J Physiol Gastrointest Liver Physiol* 300: G929–G938, 2011. First published March 17, 2011; doi:10.1152/ajpgi.00435.2010.—Inflammatory bowel diseases (IBDs), mainly Crohn's disease and ulcerative colitis, are dynamic, chronic inflammatory conditions that are associated with an increased colon cancer risk. Inflammatory cell apoptosis is a key mechanism for regulating IBD. Peptidylarginine deiminases (PADs) catalyze the posttranslational conversion of peptidylarginine to peptidylcitrulline in a calcium-dependent, irreversible reaction and mediate the effects of proinflammatory cytokines. Because PAD levels are elevated in mouse and human colitis, we hypothesized that a novel small-molecule inhibitor of the PADs, i.e., chloramidine (Cl-amidine), could suppress colitis in a dextran sulfate sodium mouse model. Results are consistent with this hypothesis, as demonstrated by the finding that Cl-amidine treatment, both prophylactic and after the onset of disease, reduced the clinical signs and symptoms of colitis, without any indication of toxic side effects. Interestingly, Cl-amidine drives apoptosis of inflammatory cells in vitro and in vivo, providing a mechanism by which Cl-amidine suppresses colitis. In total, these data help validate the PADs as therapeutic targets for the treatment of IBD and further suggest Cl-amidine as a candidate therapy for this disease.

inflammation; citrullination; apoptosis

SYSTEMIC LUPUS ERYTHEMATOSUS, rheumatoid arthritis (RA), Alzheimer's disease (AD), and inflammatory bowel disease (IBD) are autoimmune disorders that affect ~4% of the worldwide population. These diseases are heterogeneous, chronic, and relapsing inflammatory conditions that greatly impact the quality of life. Despite a wide variety of causes (e.g., environmental factors, genetic susceptibility, and imbalanced enteric bacteria), the final outcome is an abnormal immune response (i.e., loss of self-discrimination) with repeated episodes of inflammation and destruction of the surrounding tissue.

Recently, the introduction of targeted therapies that employ biological agents has improved patient outcome with these diseases. Some of the first such agents developed were TNF-α inhibitors, which are US Food and Drug Administration-approved for the treatment of RA and IBD. Such conventional symptomatic therapeutic strategies can reduce periods of active disease and help maintain remission. However, outcomes are often marginal, and there are severe side effects, including infections (e.g., tuberculosis, pneumocystosis, listeriosis, and sepsis), malignancies (e.g., lymphoma), anemia, multiple sclerosis, heart failure, occurrence of autoantibodies and autoimmunity, and injection-site reactions (19, 32, 33). Overall, there is no treatment strategy for autoimmune diseases that lacks side effects and completely inhibits the signs and symptoms of disease pathology. For this reason, new treatment strategies, targets, and/or new modulators of inflammation are necessary to battle autoimmune diseases. We have identified peptidylarginine deiminases (PADs) as one such target.

The PADs, which include five human isozymes (12), catalyze the calcium-dependent posttranslational conversion of peptidylarginine to peptidylcitrulline, and this activity is known to generate proteins with altered function or loss of function. These enzymes have drawn considerable interest in recent years, given their presumed roles in cellular differentiation, nerve growth, cell death, embryonic development, and gene transcription (downregulation of gene expression by citrullination of histones H2A, H3, and H4) (12). Additionally, dysregulated PAD activity is associated with the development of RA. For instance, autoantibodies targeting citrullinated proteins have been identified in the sera of RA patients, and these autoantibodies are present even during the asymptomatic period of RA development (37). Elevated levels of PAD enzymes and/or citrullinated proteins have also recently been found in autoimmune encephalomyelitis, obstructive nephropathy, AD, IBD, and multiple cancers, including colon cancers (3, 8, 23–26). It is very interesting to note that, in multiple sclerosis and RA, the autoantigens, e.g., fibrin, myelin basic protein, and histone H3, are citrullinated (24). Mechanistically, the deimination of these PAD substrates has been suggested to occur in response to TNF-α signaling (24). Given that anti-TNF-α monoclonal antibodies are a common treatment strategy for autoimmune diseases (i.e., IBD and RA), this finding suggests that dysregulated PAD activity may be due to inappropriate and/or uncontrolled TNF-α signaling. As such, the PAD enzyme family offers a novel, unique, and viable target for the development of a therapy that targets these diseases.

Recently, we synthesized and characterized several novel PAD inhibitors (17, 21). The most potent of these compounds, Cl-amidine, is a bioavailable haloacetamidine-based compound that inhibits all the active PAD isozymes with near equal potency (k_{inact}/K_I = 13,000 $M^{-1}\cdot min^{-1}$ for PAD4) (21). This compound has also been shown to decrease disease incidence and inhibit inflammation in the murine collagen-induced ar-

Address for reprint requests and other correspondence: L. J. Hofseth, Dept. of Pharmaceutical and Biomedical Sciences, South Carolina College of Pharmacy, Univ. of South Carolina, 770 Sumter St., Coker Life Sciences, Rm. 513C, Univ. of South Carolina, Columbia, SC 29208 (e-mail: hofseth@cop.sc.edu).

thritis model of RA, with no apparent signs of toxicity, even when given daily for 56 days at doses as high as 100 $mg \cdot kg^{-1} \cdot day^{-1}$.

Given the efficacy of Cl-amidine in the collagen-induced arthritis model and recent reports indicating that *1*) a genetic polymorphism in PAD4 is associated with increased susceptibility to ulcerative colitis (UC) (4), *2*) protein citrullination is prevalent in patients with IBD (23), and *3*) PAD enzymes are overexpressed in numerous tumors, including colon adenocarcinomas (3), we were interested in determining whether this compound could also be used to treat IBD. Here, we report that Cl-amidine treatment, both prophylactic and subsequent to the onset of disease, reduced the clinical symptoms of colitis in the dextran sulfate sodium (DSS) model. In exploring the mechanisms, we validate the PADs as a therapeutic target for the treatment of IBD and further suggest Cl-amidine as a candidate therapy for this disease.

MATERIALS AND METHODS

Cl-amidine. The synthesis of Cl-amidine has been described previously (1, 21).

DSS mouse model of colitis. C57BL/6 mice (8–12 wk old) were fed a standard AIN 93M diet, as described previously (11). For this DSS mouse model of colitis, mice received water ad libitum or 2% DSS beginning at *day 0* [for oral gavage/treatment experiment (see Supplemental Fig. S1 in Supplemental Material for this article, available at the Journal website)] or *day 7* [for intraperitoneal/prevention experiment (see Supplemental Fig. S1)]. Cl-amidine dissolved in 1× PBS or vehicle control only (1× PBS) was administrated by two methods: *1*) by intraperitoneal injections daily beginning at *day 0* (see Supplemental Fig. S1) at 75 mg/kg body wt, which is a human equivalent dose of 6.1 mg/kg daily (29), or *2*) by oral gavage (5, 25, and 75 mg/kg) daily beginning at *day 7* (see Supplemental Fig. S1). On *day 14*, blood was collected, spleens were collected, and colon samples were collected and washed with 1× PBS and processed as follows. *1*) For hematoxylin-eosin (H&E) staining and immunohistochemistry, colons were cut longitudinally, fixed in formalin, and then Swiss-rolled and embedded in paraffin, as described previously (11). *2*) Colons were flushed with 1× PBS, opened longitudinally, and cut into two pieces. Colons were incubated in 10% fetal bovine serum/5 mM ethylenediaminetetraacetic acid in Ca^{2+}/Mg^{2+}-free PBS at 37°C for 25–30 min with gentle shaking. Colon mucosal cells were then shaken to dislodge the cells and briefly pipetted up and down to generate single-cell suspensions. Inflammatory cells were isolated using $CD45^+$ magnetic microbead-positive selection according to the manufacturer's instructions (Miltenyi Biotec, Auburn, CA). Dry pellets were frozen until use for Western blot analysis. *3*) For measurement of the effects of Cl-amidine on PAD activity and citrullination in the colons, colons were removed, placed on ice, and stored at −20°C until analysis.

Quantification of inflammation. The colon was transected, pinned open, and rinsed with PBS, and the colon length was recorded. The tissue was fixed in formalin overnight, Swiss-rolled, and then embedded in paraffin, sectioned, and stained with H&E. The sections were microscopically examined for histopathological changes using the following scoring system. Histology score was determined by multiplying the percent involvement for each of the three following histological features by the percent area of involvement (16, 22). Inflammation severity was scored as 0 for none, 1 for minimal, 2 for moderate, and 3 for severe; inflammation extent as 0 for none, 1 for mucosa, 2 for mucosa and submucosa, and 3 for transmural; crypt damage as 0 for none, 1 for one-third of crypt damaged, 2 for two-thirds of crypt damaged, 3 for crypts lost and surface epithelium intact, 4 for crypts lost and surface epithelium lost; percent area involvement was scored as 0 for 0%, 1 for 1–25%, 2 for 26–50%, 3 for 51–75%, and 4 for 76–100%. Therefore, the minimal score is 0, and the maximal score is 40.

Determination of lamina propria and mesenteric lymph node cellularity. Lamina propria (LP) and mesenteric lymph node (MLN) cellularity was calculated as the total number of morphologically observed inflammatory cells within five nonoverlapping high-power fields (×400) in the LP and five nonoverlapping high-power fields (×400) in the MLN. H&E-stained sections were serially cut with sections used for PAD staining (Fig. 1*A*).

Western blot analysis. Western blot analysis was carried out as described previously (41). Antibodies include anti-p53 (polyclonal, 1:1,000 dilution; catalog no. ab3133-100, Abcam, Cambridge, MA), anti-p21 WAF1/Cip1 (monoclonal, 1:2,000 dilution, clone SX118; catalog no. M7202, Dako, Carpinteria, CA), and anti-poly(ADP-ribose) polymerase (PARP; polyclonal, 1:500 dilution; catalog no. 9542S, Cell Signaling Technology, Danvers, MA). Horseradish peroxidase (HRP)-conjugated anti-mouse and anti-rabbit secondary antibodies were purchased from Amersham. Both secondary antibodies were diluted at 1:2,000. Western blot signal was detected by Super-Signal West Pico Chemiluminescent Substrate (Thermo Scientific, Rockford, IL) and developed onto Hyperfilm (Amersham).

Immunohistochemical staining. For immunohistochemical staining, formalin-fixed, paraffin-embedded serial sections of mouse colon tissues were incubated with antibodies against pan-PAD (polyclonal, 1:20,000 dilution; catalog no. NB100-1853, Novus Biologicals, Littleton, CO), PAD2 (monoclonal, 1:10,000 dilution; catalog no. H00011240-M01, Novus Biologicals), and PAD4 (monoclonal, 1:20,000 dilution; catalog no. H00023569, Novus Biologicals). Formalin-fixed, paraffin-embedded sections from colon biopsies of human patients with colitis or normal colon biopsies from patients without colitis were incubated with the anti-pan-PAD antibody (1:5,000 dilution; catalog no. NB100-1853, Novus Biologicals). Human tissues were a kind gift from Dr. Curtis C. Harris (National Cancer Institute), with approval from the University of South Carolina Institutional Review Board. To ensure even staining and reproducible results, sections were incubated by slow rocking overnight in primary antibodies (4°C) using the Antibody Amplifier (ProHisto, Columbia, SC). After incubation with primary antibody, sections were processed using EnVision+ System-HRP kits (DakoCytomation, Carpinteria, CA) according to kit protocols, or a mouse-on-mouse kit (Vector Labs, Burlingame, CA) was used for mouse monoclonal antibodies. The chromogen was diaminobenzidine, and sections were counterstained with 1% methyl green. To ensure absolute objectivity of these immunohistochemical studies, for Fig. 1, stained tissues were examined for positivity in one of two ways: *1*) (based on percentage and intensity) by quantification with the use of the ACIS III Automated Cellular Imaging System (DakoCytomation), with the percentage of positive cells used for statistical analysis; or *2*) by a method similar to that previously described (5) with modifications. Intensity and degree of staining were evaluated independently by two blinded investigators. For each tissue section, the percentage of positive cells was scored on a scale of 0–5 for the percentage of tissue stained: 0 (0% positive cells), 1 (<10%), 2 (11–25%), 3 (26–50%), 4 (51–80%), or 5 (>80%). Staining intensity was scored on a scale of 0–3: 0 (negative staining), 1 (weak staining), 2 (moderate staining), or 3 (strong staining). The two scores were multiplied, resulting in an immunoreactivity score (IRS) value ranging from 0 to 15.

Cells. TK6 cells were a kind gift from Curtis Harris (National Cancer Institute), originally derived from the laboratories of Dr. William Thilly and Howard Liber. TK6 cells are a lymphoblastoid cell line derived from the spleen >30 years ago (34). HT29 cells are a colon cancer cell line, with mutant p53. All cells were maintained in exponentially growing suspension culture at 37°C in a humidified, 5% CO_2 atmosphere in RPMI 1640 supplemented with 10% heat-inactivated calf serum, 100 U/ml penicillin, 100 μg/ml streptomycin, and 2 mM L-glutamine.

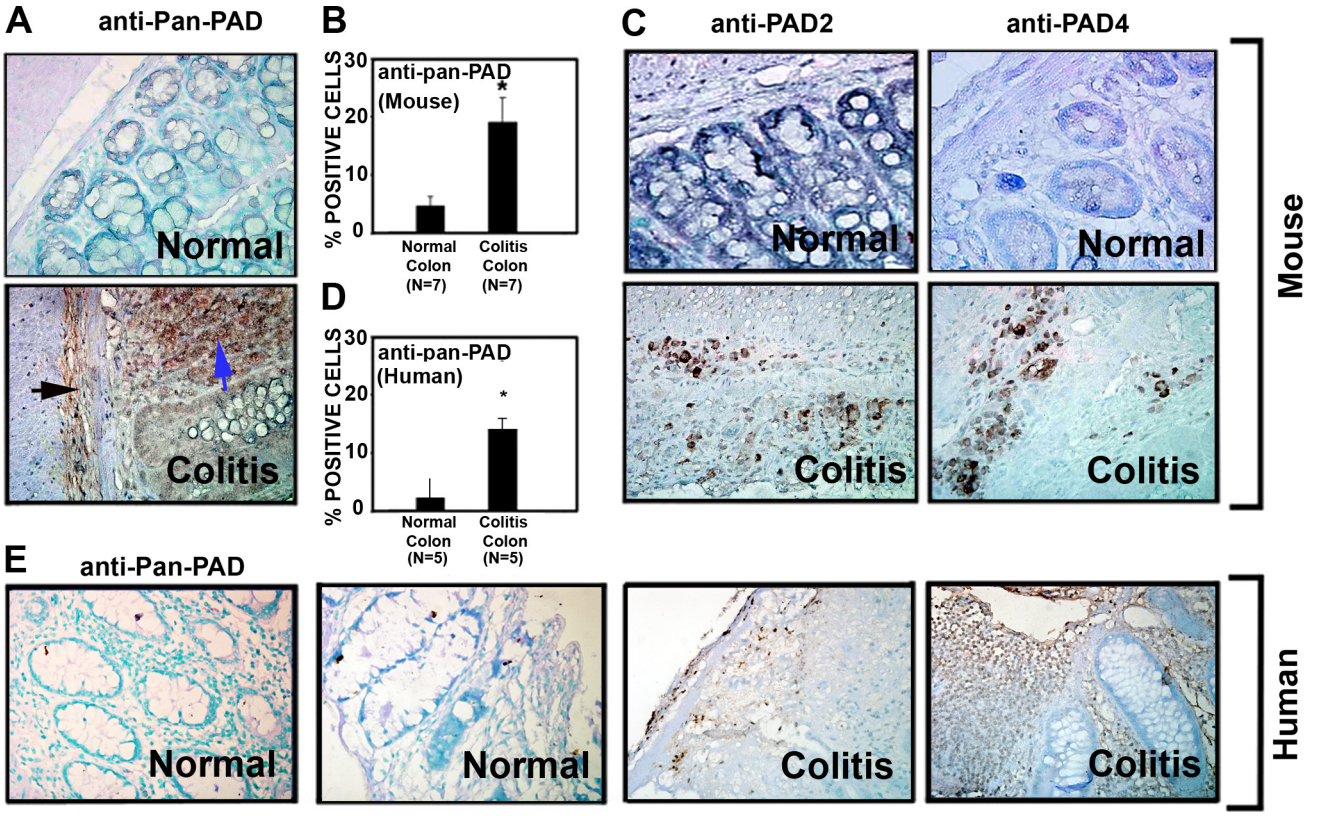

Fig. 1. Peptidylarginine deiminase (PAD) levels are elevated in mouse and human colitis. *A–C*: initial screening for which tissues archived from previous studies using the dextran sulfate sodium (DSS) mouse model of colitis were used (11, 15). Colon sections from 7 mice per group were stained (at the same time) with the polyclonal anti-pan-PAD antibody (*A*) by rocking using the Antibody Amplifier to ensure even and reproducible staining. Antibody recognizes multiple isozymes of PAD and is not specific to any 1 of the 5 known forms. Importantly, Cl-amidine is also a ubiquitous inhibitor of PAD isozymes. Staining in normal colon (*top*) was largely absent in the mucosa. In colitis (*bottom*), staining was apparent not only in inflammatory cells and the lamina submucosa (black arrow), but also in cells of the lamina propria (blue arrow). *B*: quantification with the use of an automated cellular imaging system. *Significantly increased PAD levels in colitis ($P < 0.001$). *C*: antibodies against PAD2 and PAD4 also showed increased levels of these two isozymes in mouse colon colitis tissues. *D*: quantification of human tissues [colon tissues from colitis patients with diagnostically inflamed colons ($n = 5$) and normal colon tissues from patients without colitis ($n = 5$)] by automated cellular imaging system. *Significantly increased PAD levels in colitis ($P < 0.01$). *E*: normal human colon tissue and colon tissue from patients with ulcerative colitis probed with the anti-pan-PAD antibody. Staining appears to be specific to inflammatory cells.

Flow cytometry analysis for annexin V. Cells were seeded at 1×10^6 cells/well into six-well dishes for 24 h. Then fresh medium or medium containing concanavalin A (2.5 μg/ml) was added, and the cells were cultured for 12 h. Concanavalin A was then washed off, and fresh medium (RPMI 1640 as above, but with 1% heat-inactivated calf serum) or fresh medium containing freshly dissolved indicated concentrations of Cl-amidine (0–50 μg/ml in RPMI 1640 as above, but with 1% heat-inactivated calf serum) was added for 24 h. Cells were then harvested for annexin V according to instructions provided by the kit manufacturer (BD Bioscience, San Jose, CA). Annexin V/propidium iodide staining was examined using a flow cytometer (Cytomics FC500, Beckman Coulter).

TUNEL assay. A TdT-mediated dUTP nick-end labeling (TUNEL) assay was carried out to assess apoptosis in vivo, according to the manufacturer's directions (DeadEnd Colorimetric TUNEL System, Promega, Madison, WI). Tissues used were colons collected from the experiments outlined above using Cl-amidine (75 mg/kg ip). Briefly, this modified TUNEL assay was designed to provide simple, accurate, and rapid detection of apoptotic cells in situ at the single-cell level. The system measures nuclear DNA fragmentation, an important biochemical indicator of apoptosis. It end-labels the fragmented DNA of apoptotic cells using a modified TUNEL assay. Biotinylated nucleotide is incorporated at the 3′-OH DNA ends using the enzyme terminal deoxynucleotidyl transferase. HRP-labeled streptavidin (streptavidin-HRP) is then bound to these biotinylated nucleotides, which are detected using the peroxidase substrate, hydrogen peroxide, and the stable chromogen, diaminobenzidine. With this procedure, apoptotic nuclei are stained dark brown. The counterstain was CAT Hematoxylin (Biocare Medical, Concord, CA). Labeling was carried out on serial sections from those used to score inflammatory index. TUNEL in 10 separate sections from 10 individual mice was quantified in the epithelial areas and the MLNs. For the epithelial areas, 10 random fields were evaluated per slide. Because there are fewer MLNs, we evaluated each MLN for TUNEL. Labeled tissues were examined for intensity of staining using a method similar to that previously described (7). Briefly, intensity of staining was evaluated independently by blinded investigators. For each tissue section, the percentage of positive cells in the epithelium or MLNs was given an IRS score as described for immunohistochemistry.

Measurement of PAD activity in vivo. Four mice were used, and the DSS mouse model of colitis was carried out as described above. Groups were treated with water, 2% DSS, or 2% DSS + 75 mg/kg ip beginning on *day 0* (see Supplemental Fig. S1). On *day 14*, the entire colon and spleen were put on ice and stored at −20°C until analysis. Samples were resuspended into a resuspension buffer [50 mM HEPES (pH 7.6), 2 mM DTT, 1 mM PMSF, 1% Nonidet P40, and 10% glycerol] and homogenized using a glass Dounce tissue homogenizer. Lysates were then centrifuged at 13,400 *g* for 30 min at 4°C. The supernatant was separated, and the protein concentration was determined using the Lowry method. PAD activity in samples was mea-

sured using a previously described PAD activity assay (13). Briefly, 20 μl of each sample were added to a reaction buffer containing 50 mM NaCl, 10 mM $CaCl_2$, 2 mM DTT, 100 mM Tris (pH 7.6), and 10 mM *N-R*-benzoyl L-arginine ethyl ester. The reaction was performed in duplicate and allowed to proceed for 2 h before being frozen in liquid nitrogen. A color development solution that detects citrullinated proteins [COLDER; 200 μl (14)] was then added. The sample was vortexed and incubated at 95°C for 30 min. The absorbance at 540 nm was then measured and compared with a standard curve of known citrulline concentrations. The data were normalized using the protein concentrations for each sample, and these values were subtracted from a sample blank to account for residual citrullinated proteins. To measure the amount of peptidylcitrulline in the samples, tissue lysates were first desalted using PD MiniTrap Sephadex G-10 columns (GE Healthcare). Briefly, homogenized tissue lysates (100–300 μl) were applied to the columns, and proteins were eluted with sterile double-distilled H_2O (500 μl). Protein concentration of the desalted tissue samples was measured using the DC Protein Assay (Bio-Rad). Total citrulline content was measured by reacting 60 μl of the desalted samples with 200 μl of COLDER solution. The plate was incubated at 95°C for 30 min and measured as described previously (13). The background was subtracted using a sample of resuspension buffer, and the data were normalized using the protein concentrations for each sample.

Statistics. Mean differences between groups were compared by one-way ANOVA with Scheffé's multiple comparison tests. A Pearson correlation coefficient was applied for comparisons of the trends. $P = 0.05$ was chosen for significance.

RESULTS

PAD levels are elevated in mouse and human colitis. Given that recent studies have demonstrated that increased protein citrullination is apparent in human IBD (23), we wished to confirm that PAD levels were also increased in the colonic inflammatory lesions present in DSS-induced colitis. For these experiments, we used tissues archived from previous studies using the DSS mouse model of colitis (11, 15). The relative amount of PAD enzyme in this tissue was detected using a polyclonal anti-pan-PAD antibody that recognizes all five PAD isozymes (Fig. 1*A*). Staining in normal mouse colon (Fig. 1*A*, *top*) was largely absent in the mucosa. In mouse colitis (Fig. 1*A, bottom*), staining was apparent not only in inflammatory cells and the lamina submucosa, but also in mucosal epithelial cells. Quantification of these data (Fig. 1*B*) indicates a significant increase in PAD levels in DSS-induced colitis ($P < 0.001$). Given that PAD2 and PAD4 are known to be expressed in immune cells, we next used immunohistochemistry to determine whether the levels of one, or both, of these isozymes were elevated in these tissues. The results indicate that the levels of both of these enzymes are increased in mouse colon colitis tissues (Fig. 1*C*).

Although DSS-induced colitis is an accepted animal model of human colitis, we wished to confirm the relevance of these findings to the situation in human IBD. Therefore, we used the same anti-pan-PAD antibody to demonstrate that PAD levels are elevated in affected colon tissue from patients with UC compared with normal colon tissue (Fig. 1, *D* and *E*). Staining appears to be specific to inflammatory cells in the human UC tissues. Interestingly, there was a significant correlation ($r = 0.89$, $P < 0.05$) between the percentage of cells positive for PAD (anti-pan-PAD slides were evaluated) and the total estimated number of inflammatory cells (in MLN and LP) in a serial H&E-stained section (see Supplemental Fig. S2). In total, these studies demonstrate that PAD levels are increased in human UC patients and DSS-induced mouse colitis, thereby helping validate the use of PAD inhibitors, such as Cl-amidine, as a potential treatment for this disease.

Cl-amidine suppresses and treats DSS-induced colitis. To explore whether PAD inhibition represents a viable approach to the treatment of IBD, we set out to determine whether Cl-amidine, a pan-PAD inhibitor, could inhibit colon inflammation in DSS-induced colitis. Initial experiments used injections of Cl-amidine (75 $mg \cdot kg^{-1} \cdot day^{-1}$ ip), beginning concomitantly with the initiation of 2% DSS in the drinking water. This dose was chosen based on results in a RA model that used ≤ 100 $mg \cdot kg^{-1} \cdot day^{-1}$ without overt side effects and without immunosuppressive outcomes. In our DSS model, 50 mice in 4 groups were examined, and inflammation scores were recorded as described in MATERIALS AND METHODS. Figure 2*A* shows significantly higher levels of colon inflammation in the 2% DSS than the 2% DSS + Cl-amidine mice ($P < 0.05$). The mean histology scores were 24.2 ± 1.7 (SE) and 13.9 ± 1.6, respectively. Most of the damage in the DSS-only group was in the distal colon, and this damage was suppressed with DSS + Cl-amidine.

Because mouse colon length decreases in an inflamed state (10, 11), we also used this end point as a metric for inflammation severity. For the DSS-treated group, the mean colon length was 7.2 ± 0.2 cm. In contrast, the average colon length of the DSS + Cl-amidine group was 8.4 ± 0.2 cm, which is comparable to the mean colon lengths obtained for the water-alone and water + Cl-amidine groups (8.4 ± 0.3 and 7.9 ± 0.2 cm, respectively). These results indicate that Cl-amidine prevents the DSS-induced decrease in colon length and are consistent with the histology scores.

In addition to these end points, we also measured the total distance and average speed of mice over a 96-h period (see Supplemental Fig. S3). The results of these analyses demonstrated that the total distance was 5,072 ± 381 and 3,190 ± 401 m for the water-treated and DSS + Cl-amidine mice, but only 800 ± 163 m for the DSS-only group. Similarly, the average speed on the wheel over the 4-day period was 6.2 ± 0.63 and 5.3 ± 0.58 m/min for the water-treated and DSS + Cl-amidine groups, but only 1.8 ± 0.51 m/min for the DSS group. Representative movies showing the overall movements of these mice are available as supplemental material (see Supplemental Movies 1–3). The finding that Cl-amidine improves the speed and distance traveled by the mice is consistent with the histology and colon length data and demonstrates overall improved health, further demonstrating the efficacy of this compound in treating DSS-induced colitis.

Gross toxicity of Cl-amidine. To evaluate the gross toxicity of Cl-amidine, several end points, including number of animal deaths, gross necroscopy, weight, and white blood cell (WBC) counts, were examined. *1*) No animals died during the study, regardless of treatment. *2*) No gross abnormalities were observed in tissues obtained from the Cl-amidine (water + Cl-amidine and DSS + Cl-amidine) groups. *3*) The water + Cl-amidine group gained more weight than the water-only group (4.1 ± 0.7 vs. 2.8 ± 0.4 g). This was an interesting finding that may suggest an impact of Cl-amidine on lipid metabolism. Further experiments are needed to follow up on this hypothesis. *4*) Total WBC counts between the water-treated and water + Cl-amidine groups did not differ signifi-

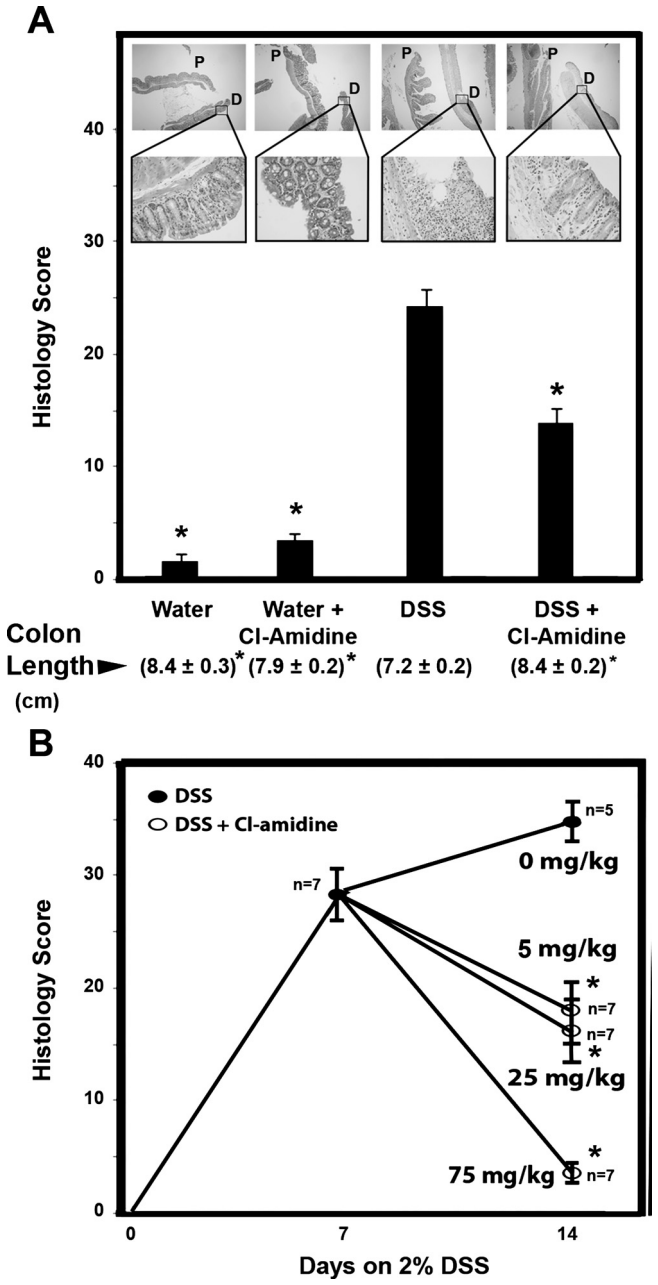

Fig. 2. Cl-amidine suppresses and reverses DSS-induced colitis in mice. *A*: histological score is lower in mice injected intraperitoneally with Cl-amidine concomitant with DSS than in mice consuming DSS alone. Values are means ± SE of 10 mice/group for water and water + Cl-amidine (75 mg/kg) and 15 mice/group for DSS and DSS + Cl-amidine. Values in parentheses are colon lengths (means ± SE). *Significantly different from DSS group ($P < 0.05$). Representative hematoxylin-eosin (H&E)-stained colons are shown for each group [×40 magnification (*top*) and ×400 magnification (*bottom*)]. *P*, proximal colon; D, distal colon. Arrow for the DSS group indicates an area of mucosal ulceration. *B*: treatment of DSS-induced colitis by Cl-amidine (daily oral gavage) in a dose-response manner. Values are means ± SE for 7 mice each group. *Significantly different from 2% DSS alone (0 mg/kg Cl-amidine corresponds to vehicle alone, which is PBS). For scoring, sections were stained with H&E. Sections were microscopically examined for histopathological and inflammatory changes using a histology scoring system, which consisted of multiplying percent involvement for 3 histological features [inflammation severity (0–3), inflammation extent (0–3), and crypt damage (0–4)] by percent area [0% (0), 1–25% (1), 26–50% (2), 51–75% (3), >75% (4)] of involvement, as previously described (10, 22).

cantly (5,100 ± 600 and 5,900 ± 400 WBCs/μl, respectively). Overall, these results suggest that Cl-amidine can suppress DSS-induced inflammation in the colon, with no observable immunosuppressive or toxic side effects.

Oral Cl-amidine suppresses colitis in a dose-dependent manner after the onset of colitis. To investigate the efficacy of Cl-amidine under a more clinical model, we examined the dose-dependent effects of Cl-amidine given by oral gavage after the onset of colitis. Figure 2*B* shows, in mice consuming 2% DSS for 1 wk, a moderate degree of colon inflammation, as reflected by the histology score of 28.4 ± 1.9. When mice were continued on 2% DSS for an additional week, the degree of colon inflammation became severe, with a histology score of 34.8 ± 1.4. In fact, two mice from this group died from bowel perforation and sepsis. However, mice consuming 2% DSS concomitantly with Cl-amidine showed reduced colon inflammation in a dose-dependent manner. Cl-amidine (5 $mg \cdot kg^{-1} \cdot day^{-1}$) + 2% DSS prevented additional colon inflammation beyond that observed at 1 wk in the 2% DSS group; the histology score was only 17.4 ± 3.7 vs. 28.4 ± 1.9 at the end of *week 1*. At the higher doses, i.e., 25 and 75 $mg \cdot kg^{-1} \cdot day^{-1}$, Cl-amidine led to even more significant reductions in the histology scores (15.5 ± 2.3 and 3.1 ± 0.3, respectively). Table 1 outlines gross characteristics that support the histological findings. From these data, it is apparent that Cl-amidine prevents weight loss, colon shrinkage, and elevated WBC counts; increases in these end points are hallmarks of an unhealthy mouse. It is especially noteworthy that the WBC count for the Cl-amidine groups does not change significantly from that for the water-treated group, indicating that Cl-amidine lacks a generalized immunosuppressive effect. Also, in the 2% DSS-only 1-wk group, although there was a reduction in body weight and colon length (as well as an elevation in colon inflammation) compared with the water-treated group, there was no change in systemic WBC count. One possibility for this finding is that although colitis is evident at this time point, there is not enough bowel erosion caused by the DSS challenge to contribute significantly to systemic inflammation at the 1-wk time period. Such a lack of elevated systemic inflammation at acute DSS challenges has been shown by other groups (35).

Cl-amidine suppresses PAD activity, protein citrullination, and PAD levels in vivo. To further confirm that the efficacy of Cl-amidine is due to its ability to inhibit PAD activity, we assayed PAD activity and total protein citrullination in whole colons and spleens isolated during experiments outlined in Fig. 1*A* and described in MATERIALS AND METHODS. The spleen was examined to evaluate the systemic effects of Cl-amidine. Note that these experiments are possible, because Cl-amidine irreversibly inactivates the PADs by forming a covalent adduct with an active site cysteine residue that is critical for catalysis; thus there is no washout or dilution of the inhibitor during cell lysis and activity assay. The results indicate that PAD activity was significantly increased in the colons of mice treated with DSS, relative to the water-treated and DSS + Cl-amidine groups (Fig. 3*A*). The levels of protein citrullination were consistent with these data (Figs. 3*B*), further suggesting that Cl-amidine derives its efficacy from its ability to inhibit the deiminating activity of the PADs. To rule out that Cl-amidine targets free citrulline, the tissue samples were desalted using PD MiniTrap Sephadex G-10 columns (GE Healthcare), and the total peptidylcitrulline was content measured; the exclusion

Table 1. *Gross characteristics of treated groups*

Treatment	Weight Change, g	Colon Length, cm	WBC Count, m/mm^3†
Water	1.12 ± 0.46*	8.6 ± 0.23*	9.5 ± 0.7*
2% DSS only			
1 wk	−3.27 ± 0.98*	6.89 ± 0.45*	7.95 ± 0.91*
2 wk	−8.85 ± 0.65	5.2 ± 0.1	26.76 ± 1.87
2% DSS + 5 mg/kg Cl-amidine	−2.19 ± 0.76*	7.54 ± 0.52*	7.97 ± 0.95*
2% DSS + 25 mg/kg Cl-amidine	−2.13 ± 0.81*	7.89 ± 0.25*	9.31 ± 0.75*
2% DSS + 75 mg/kg Cl-amidine	−0.40 ± 0.47*	9.56 ± 0.22*	7.85 ± 0.65*

Values are means ± SE. Groups treated with 2% dextran sulfate sodium (DSS) + Cl-amidine were treated for 1 wk with 2% DSS only and then for 1 wk with 2% DSS + Cl-amidine (5, 25, or 75 mg/kg). WBC, white blood cell. *Significantly different from 2% DSS only (2 wk). †Millions per cubic milliliter of blood.

limit for Sephadex G-10 is 700 Da; thus free citrulline was retained on the resin, and the eluate will contain peptidylcitrulline. As is apparent in Fig. 3*C*, Cl-amidine treatment decreases peptidylcitrulline content in the colons relative to treatment with DSS only. These data are consistent with data obtained when total citrulline content was measured. These data are also consistent with the notion that Cl-amidine exerts its effects via its ability to inhibit PAD activity, which we have also demonstrated to occur in these tissues. To determine if Cl-amidine also suppressed PAD levels, we probed for PAD using a pan-PAD antibody. Figure 3*D* shows that the IRS of PAD was elevated with DSS treatment and suppressed by the use of Cl-amidine concomitantly with DSS. Figure 3*E* shows representative sections.

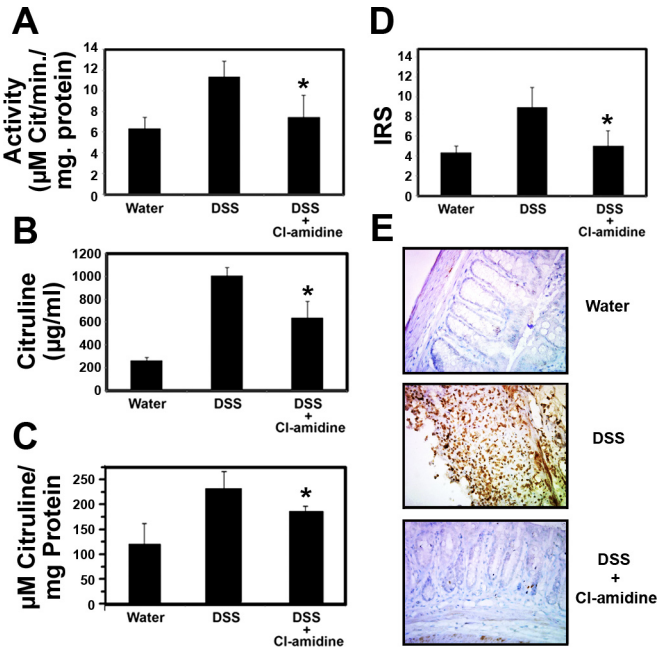

Fig. 3. Cl-amidine suppresses PAD activity, protein citrullination, and PAD levels in the colon in vivo. *A*: PAD activity is significantly reduced in mice treated with DSS + Cl-amidine (75 mg/kg ip) compared with the DSS-treated group (n = 4 in each group). *B*: citrulline levels are significantly reduced in mice treated with DSS + Cl-amidine (75 mg/kg ip) compared with the DSS-treated group (n = 4 in each group). *C*: peptidylcitrulline content in the colons is significantly reduced in mice treated with DSS + Cl-amidine (75 mg/kg ip) compared with the DSS-treated group (n = 4 in each group). *D*: PAD levels [quantified by immunoreactivity score (IRS) in pan-PAD-stained tissues] are significantly reduced in mice treated with DSS + Cl-amidine (75 mg/kg ip) compared with the DSS-treated group [n = 8, 9, and 10 for water, DSS, and DSS + Cl-amidine (75 mg/kg ip), respectively]. *Significantly different from DSS alone. *E*: representative pan-PAD-stained tissues from each group (×400 magnification).

Similar effects on PAD activity were observed in tissues from the spleen; i.e., PAD activity was significantly increased in DSS-treated mice relative to the water-treated and DSS + Cl-amidine groups (see Supplemental Fig. S4*A*). In contrast to the citrullination data for the colon, this end point was unchanged in the spleens from all groups (see Supplemental Fig. 4, *B* and *C*). This result is consistent with the hypothesis that although spleen inflammatory cells contain increased PAD levels (due to the increase in inflammatory/immune cell content in this organ in the DSS model), the enzymes are not activated in spleens, and as such, there is no increase in protein citrullination in this tissue. The decreased PAD activity is either associated with inhibition of activated immune cells in the inflamed tissues that migrate back to the spleen or, alternatively, inhibition of nonactivated PADs in the spleens themselves. The latter option is possible, because Cl-amidine will covalently modify the PADs in the absence of calcium, albeit at reduced levels. Note that it is possible to observe these effects, because the PADs are not activated until after cell lysis and the addition of calcium, which is required to observe PAD activity in vitro.

Cl-amidine causes apoptosis of inflammatory cells in vitro. Colitis is associated with heavy infiltration of inflammatory cells into the colon, and apoptosis of such cells is a key mechanism toward regulating this disease (27, 30). Because elevated PAD levels have been observed in inflammatory cells (Fig. 1) and because we previously showed that inactivation of PAD enzymes by Cl-amidine can induce apoptosis in cancer cells (18), we hypothesized that Cl-amidine may target inflammatory cells for apoptosis. To test this hypothesis, we examined whether Cl-amidine could induce apoptosis of TK6 cells, a lymphoblastoid cell line. Figure 4*A* and Supplemental Fig. S5 show that Cl-amidine induces apoptosis (identified as annexin V-positive/propidium iodide-negative cells) in such cells in a dose-dependent manner, indicating that Cl-amidine induces apoptosis of WBCs in vitro. Interestingly, the colon cancer cell line (HT29) is relatively resistant to apoptosis caused by Cl-amidine (Fig. 4*B*).

Cl-amidine stimulates apoptosis of inflammatory cells in vivo. To examine the effects of Cl-amidine on apoptosis in vivo, we carried out a TUNEL assay on serial tissue sections obtained from mice treated with water, DSS, or DSS + 75 mg·kg^{-1}·day^{-1} Cl-amidine. These are groups taken from experiments outlined for Fig. 1*A*. The results demonstrate that, for epithelial cells, IRS (i.e., TUNEL label) was significantly

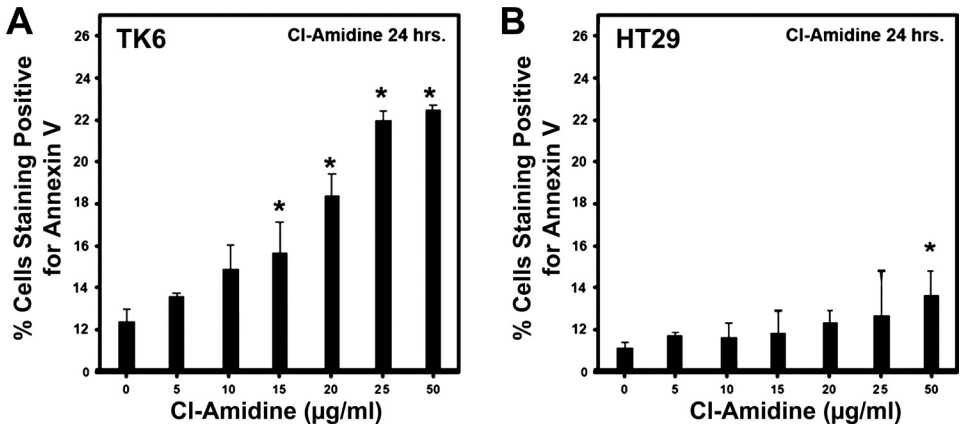

Fig. 4. TK6 lymphoblastoid cells and HT29 colon cancer cells were cultured with Cl-amidine in a dose-dependent manner over 24 h. *A*: lymphocyte cell lines undergo apoptosis in response to Cl-amidine treatment. *B*: colon cancer cell lines are relatively resistant to effects of Cl-amidine treatment. Apoptosis was assessed by annexin V/propidium iodide staining followed by flow cytometry. *Significant increase from control (0 μg/ml).

higher in DSS- than water-treated mice (Fig. 5). With DSS + Cl-amidine, the TUNEL IRS in the epithelial cells is significantly decreased relative to epithelial cells treated with DSS only, indicating less damage to this cell type. Labeling only occurs on the surface epithelium in the water-treated and DSS + Cl-amidine groups but appears to label more crypt cells toward the basal layer in the DSS group, indicating more widespread apoptosis in this group (Fig. 5*A*). This observation is consistent with the data from the inflammatory index (Fig. 2*A*), indicating that Cl-amidine protects epithelial cells from DNA damage in vivo. We should note here, also, that there is abundant positive TUNEL staining in the LP lymphocytes in the DSS group, with the level of staining extensively reduced in the DSS + Cl-amidine group. This observation is consistent with the understanding that there are fewer LP lymphocytes in the latter group because of the actions of Cl-amidine. There was a slight increase in IRS in the inflammatory cells of the MLNs treated with DSS alone. However, with DSS + Cl-amidine treatment, the TUNEL IRS was significantly elevated. Such results are consistent with our in vitro data and with the hypothesis that Cl-amidine drives apoptosis of MLN inflammatory cells in vivo. To begin exploring the mechanisms, following treatment with water, 1% DSS, 1% DSS + Cl-amidine (75 mg/kg ip), or 1% DSS + Cl-amidine (75 mg/kg po), we isolated colonic mucosal cells. After separation of inflammatory cells ($CD45^+$), we examined the effects of treatment on p53 levels and downstream targets associated with proliferation and apoptosis. Figure 6 indicates that, in $CD45^+$ inflammatory cells, there is a small induction of p53 in the DSS-only group, which we showed previously (5, 10, 11). Interestingly, however, p53 levels were elevated more in both DSS + Cl-amidine groups, with the highest levels in the groups treated with Cl-amidine given by oral gavage. p21 levels were increased parallel with p53 levels, indicating inhibition of inflammatory cell cycle. Finally, PARP cleavage was detected in the group given DSS + Cl-amidine by oral gavage, consistent with TUNEL results.

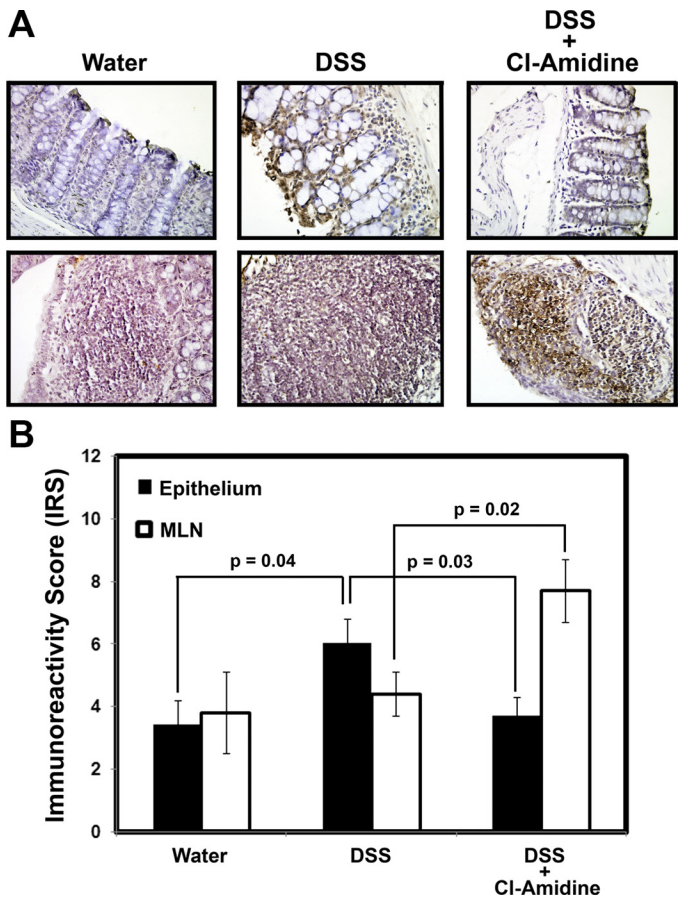

Fig. 5. Cl-amidine increases apoptosis of mesenteric lymph node (MLN) inflammatory cells in DSS-induced colitis. Mice were treated with water, DSS, or DSS + Cl-amidine (75 mg/kg ip), as described in Fig. 2*A*. *A*: representative staining in epithelium (*top*) and MLN (*bottom*). *B*: quantification of staining (IRS); $n = 8$ water-treated mice, $n = 14$ DSS-treated mice, $n = 14$ DSS + Cl-amidine-treated mice. For each tissue section, IRS indicates percentage of positive cells in epithelium or MLN.

DISCUSSION

We have shown that Cl-amidine, a small-molecule PAD inhibitor, can prevent and treat DSS-induced colitis. Mechanistically, this appears to be, at least in part, through the stimulation of inflammatory cell apoptosis. We also note that Cl-amidine does not appear to target the normal colon epithelium for apoptosis (Fig. 5). In fact, Cl-amidine appears to specifically target the inflammatory cell population in vitro (Fig. 4) and in vivo (Fig. 5). The finding that the normal colon epithelium remains intact with less apoptosis following Cl-amidine is most likely secondary to the reduction in inflammation caused by targeting of inflammatory cells for apoptosis. However, we cannot rule out a direct effect of Cl-amidine in

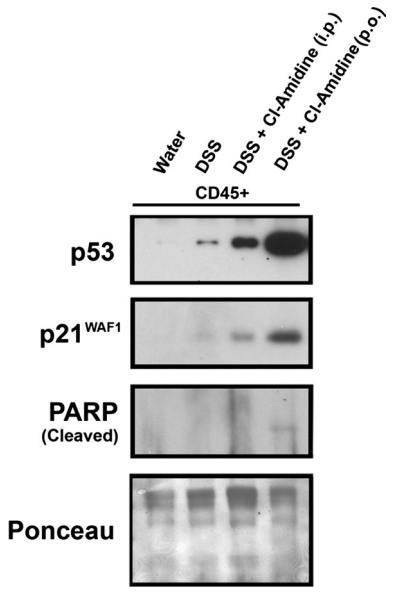

Fig. 6. Cl-amidine causes an induction of p53 in CD45$^+$ inflammatory cells. Mice were treated with water, 1% DSS, 1% DSS + Cl-amidine (75 mg/kg ip), or 1% DSS + Cl-amidine (75 mg/kg po). p53 was induced by Cl-amidine above that of DSS alone by both routes of administration. There was a concomitant increase in the p53 target and cell cycle inhibitor p21^{WAF1}. There was also detectable poly(ADP-ribose) polymerase (PARP) cleavage in the group treated with DSS + Cl-amidine (75 mg/kg po). Levels of protein loaded were similar, as indicated by Ponceau staining.

the protection of normal colonic epithelial cells. Because of the lack of availability of normal colonic epithelial cells, this hypothesis will be difficult to explore. However, initial experiments presented here (Fig. 4) indicate that Cl-amidine preferentially targets inflammatory cells over colon cancer cell lines for apoptosis. To this end, we recently showed that PAD4 inhibition can induce apoptosis in the colon cancer cell line HCT116 (p53 wild-type), but not in isogenic p53-deficient HCT116 cells (18). Of note here is that the colon cancer cells used in our study (HT29) are p53 mutant. Given that p53 is a key molecule mutated in colitis and colon cancer associated with colitis (10), this may be a significant observation that will be followed up in future studies. Initial experiments indicate that the p53 pathway may be involved, not only in Cl-amidine-induced apoptosis, but also in Cl-amidine-induced cell cycle arrest in CD45$^+$ inflammatory cells isolated from the colons of treated mice (Fig. 6). This is because Cl-amidine dramatically elevates p53 levels (especially when given orally) in the inflammatory cells above that of the DSS-only group. The latter group presumably has elevated p53 due to stressed and activated inflammatory cells. This dramatic increase in p53 levels correlates with an upregulation of the p53 target and cell cycle inhibitor p21^{WAF1} and with PARP cleavage. We note, however, that it is also possible that additional molecules may explain the relative difference in susceptibility to apoptosis in inflammatory cells vs. epithelial cells. Such pathways will be examined in detail in separate studies to understand the underpinnings of Cl-amidine-induced apoptosis and/or cell cycle arrest of inflammatory cells as a mechanism relevant to its ability to treat colitis.

Nevertheless, our findings make Cl-amidine an exciting therapeutic candidate for the treatment of colitis, as Cl-amidine also appears to lack any significant toxicity. Consistent with this notion, we did not observe any general immunosuppressive effects by Cl-amidine. This characteristic is somewhat unique in current treatment strategies for colitis, as, for example, 5-aminosalicylates, which are the standard treatment for mild-to-moderate colitis (28), possess a number of side effects, including headache, diarrhea, and rash (28).

We recognize that these studies are preclinical, and there remains an extensive amount of investigation to determine whether Cl-amidine will work to inhibit IBD in humans. Nevertheless, the evidence, so far, suggests that PAD inhibition with Cl-amidine represents a viable treatment strategy for humans. This is likely to be true because, for example, increased PAD levels and/or citrullination have been observed in the inflammatory lesions present in the colons of patients with IBD (23, 36) (Fig. 1). Consistent with the fact that PADs are expressed in inflammatory cells is our observation that PAD staining occurs mainly in inflammatory cells in colitis patients (Fig. 1). We have further shown that PAD2 and PAD4 are specifically overexpressed in the colons of mice with DSS-induced colitis, consistent with the understanding that these two isozymes are the predominant PADs expressed in inflammatory cells (8).

Also consistent with a role for elevated PAD activity in IBD is the recent identification of a PAD4 haplotype present in a Japanese population and associated with an increased susceptibility for developing Crohn's disease (4). Although this haplotype does not alter the amino acid sequence of PAD4 and the specific effect of this haplotype on PAD activity and/or expression is unknown, it is also interesting to note that the PAD4 gene (i.e., *PADI4*) lies within the IBD-susceptibility locus. With respect to colon cancer, it is also noteworthy that PAD enzyme levels have been reported to be increased in tumors, including colon adenocarcinomas (2).

Given our data, it is clear that dysregulated PAD activity contributes to the onset and progression of colitis and that PAD inhibition represents a potential strategy for the treatment of this disease. However, because of the novelty of these findings, it is difficult to speculate on the mechanisms by which these enzymes contribute to colitis. Furthermore, the identities of the proteins being citrullinated in this disease and how these contribute to disease progression are unknown. Nevertheless, our results showing that dysregulated PAD activity occurs in colitis and that Cl-amidine can reverse colitis parallel recent findings showing that elevated citrullination is associated with a number of other inflammatory diseases, including arthritis (38), multiple sclerosis (25), and AD (9, 31). For example, increased PAD2 expression and citrullinated myelin basic protein have long been associated with multiple sclerosis (25). Similar results have been observed in AD patients, where PAD2 levels and generalized citrullination are elevated in the hippocampus (9).

In addition to IBD, MS, and AD, dysregulated PAD activity is highly correlated with the onset and progression of RA. For example, in RA, autoantibodies targeting citrullinated protein antigens (ACPA) are present in the sera of individuals who ultimately develop seropositive RA for an average of 4–5 yr prior to the onset of clinically apparent disease (6), and these autoantibodies are the most specific diagnostics for RA (20, 39). Additionally, elevated levels of PAD2 and PAD4, as well as citrullinated proteins, are present in the joints of patients

with RA, and higher levels of these proteins correlate with a more erosive form of the disease (12). A PAD4 haplotype is also highly associated with an increased susceptibility of developing RA in Asian populations (40). Finally, Cl-amidine has been shown to reduce disease severity in the murine collagen-induced arthritis model of RA. In combination, these results suggest that dysregulated PAD activity is a hallmark of inflammatory diseases. Although ACPAs have not been detected in most inflammatory diseases, a recent report suggests that such autoantibodies are also present in patients with dementia of Alzheimer's type (31). Thus it would be interesting to determine whether ACPAs are also present in IBD. In total, our observations highlight a potential role for dysregulated (i.e., increased) PAD activity in the onset and progression of colitis. Our findings that the PAD inhibitor Cl-amidine suppresses and can be used to treat colitis in mice support a new approach to the treatment of this debilitating disease associated with a high colon cancer risk.

ACKNOWLEDGMENTS

Contact information for P. R. Thompson: Dept of Chemistry, The Scripps Research Institute, Scripps Florida, 130 Scripps Way, Jupiter, FL 33458 (e-mail: pthompso@scripps.edu).

GRANTS

This work was supported by National Institutes of Health Center for Colon Cancer Research Grant 5P20 RR-017698-08 (L. J. Hofseth, P. R. Thompson, and L. E. Matesic) and in part by Grant GM-079357 (P. R. Thompson) and by National Institutes of Health Grants 1R01CA151304–01A1 and 1R01CA151304.

DISCLOSURES

No conflicts of interest, financial or otherwise, are declared by the authors.

REFERENCES

1. **Causey CP, Thompson PR.** An improved synthesis of haloaceteamidine-based inactivators of protein arginine deiminase 4 (PAD4). *Tetrahedron Lett* 49: 4383–4385, 2008.
2. **Chang X, Han J.** Expression of peptidylarginine deiminase type 4 (PAD4) in various tumors. *Mol Carcinog* 45: 183–196, 2006.
3. **Chang X, Han J, Pang L, Zhao Y, Yang Y, Shen Z.** Increased PADI4 expression in blood and tissues of patients with malignant tumors. *BMC Cancer* 9: 40, 2009.
4. **Chen CC, Isomoto H, Narumi Y, Sato K, Oishi Y, Kobayashi T, Yanagihara K, Mizuta Y, Kohno S, Tsukamoto K.** Haplotypes of PADI4 susceptible to rheumatoid arthritis are also associated with ulcerative colitis in the Japanese population. *Clin Immunol* 126: 165–171, 2008.
5. **Cui X, Jin Y, Hofseth AB, Pena E, Habiger J, Chumanevich A, Poudyal D, Nagarkatti M, Nagarkatti PS, Singh UP, Hofseth LJ.** Resveratrol suppresses colitis and colon cancer associated with colitis. *Cancer Prev Res* 3: 549–559, 2010.
6. **De Rycke L, Peene I, Hoffman IE, Kruithof E, Union A, Meheus L, Lebeer K, Wyns B, Vincent C, Mielants H, Boullart L, Serre G, Veys EM, De Keyser F.** Rheumatoid factor and anticitrullinated protein antibodies in rheumatoid arthritis: diagnostic value, associations with radiological progression rate, and extra-articular manifestations. *Ann Rheum Dis* 63: 1587–1593, 2004.
7. **Denkert C, Koch I, von Keyserlingk N, Noske A, Niesporek S, Dietel M, Weichert W.** Expression of the ELAV-like protein HuR in human colon cancer: association with tumor stage and cyclooxygenase-2. *Mod Pathol* 19: 1261–1269, 2006.
8. **Foulquier C, Sebbag M, Clavel C, Chapuy-Regaud S, Al Badine R, Mechin MC, Vincent C, Nachat R, Yamada M, Takahara H, Simon M, Guerrin M, Serre G.** Peptidyl arginine deiminase type 2 (PAD-2) and PAD-4 but not PAD-1, PAD-3, and PAD-6 are expressed in rheumatoid arthritis synovium in close association with tissue inflammation. *Arthritis Rheum* 56: 3541–3553, 2007.
9. **Ishigami A, Ohsawa T, Hiratsuka M, Taguchi H, Kobayashi S, Saito Y, Murayama S, Asaga H, Toda T, Kimura N, Maruyama N.** Abnormal accumulation of citrullinated proteins catalyzed by peptidylarginine deiminase in hippocampal extracts from patients with Alzheimer's disease. *J Neurosci Res* 80: 120–128, 2005.
10. **Jin Y, Hofseth AB, Cui X, Windust AJ, Poudyal D, Chumanevich AA, Matesic LE, Singh NP, Nagarkatti M, Nagarkatti PS, Hofseth LJ.** American ginseng suppresses colitis through p53-mediated apoptosis of inflammatory cells. *Cancer Prev Res* 3: 339–347, 2010.
11. **Jin Y, Kotakadi VS, Ying L, Hofseth AB, Cui X, Wood PA, Windust A, Matesic LE, Pena EA, Chiuzan C, Singh NP, Nagarkatti M, Nagarkatti PS, Wargovich MJ, Hofseth LJ.** American ginseng suppresses inflammation and DNA damage associated with mouse colitis. *Carcinogenesis* 29: 2351–2359, 2008.
12. **Jones JE, Causey CP, Knuckley B, Slack-Noyes JL, Thompson PR.** Protein arginine deiminase 4 (PAD4): current understanding and future therapeutic potential. *Curr Opin Drug Discov Dev* 12: 616–627, 2009.
13. **Kearney PL, Bhatia M, Jones NG, Yuan L, Glascock MC, Catchings KL, Yamada M, Thompson PR.** Kinetic characterization of protein arginine deiminase 4: a transcriptional corepressor implicated in the onset and progression of rheumatoid arthritis. *Biochemistry* 44: 10570–10582, 2005.
14. **Knipp M, Vasak M.** A colorimetric 96-well microtiter plate assay for the determination of enzymatically formed citrulline. *Anal Biochem* 286: 257–264, 2000.
15. **Kotakadi VS, Jin Y, Hofseth AB, Ying L, Cui X, Volate S, Chumanevich A, Wood PA, Price RL, McNeal A, Singh UP, Singh NP, Nagarkatti M, Nagarkatti PS, Matesic LE, Auclair K, Wargovich MJ, Hofseth LJ.** Ginkgo biloba extract EGb 761 has anti-inflammatory properties and ameliorates colitis in mice by driving effector T cell apoptosis. *Carcinogenesis* 29: 1799–1806, 2008.
16. **Krieglstein CF, Cerwinka WH, Laroux FS, Grisham MB, Schurmann G, Bruwer M, Granger DN.** Role of appendix and spleen in experimental colitis. *J Surg Res* 101: 166–175, 2001.
17. **Kunckley B, Causey CP, Pellechia PJ, Cook PF, Thompson PR.** Haloacetamidine-based inactivators of protein arginine deiminase 4 (PAD4): evidence that general acid catalysis promotes efficient inactivation. *Chembiochem* 11: 11, 2009.
18. **Li P, Yao H, Zhang Z, Li M, Luo Y, Thompson PR, Gilmour DS, Wang Y.** Regulation of p53 target gene expression by peptidylarginine deiminase 4. *Mol Cell Biol* 28: 4745–4758, 2008.
19. **Lichtenstein GR, Abreu MT, Cohen R, Tremaine W.** American Gastroenterological Association Institute technical review on corticosteroids, immunomodulators, and infliximab in inflammatory bowel disease. *Gastroenterology* 130: 940–987, 2006.
20. **Lopez-Longo FJ, Sanchez-Ramon S, Carreno L.** The value of anticyclic citrullinated peptide antibodies in rheumatoid arthritis: do they imply new risk factors? *Drug News Perspect* 22: 543–548, 2009.
21. **Luo Y, Arita K, Bhatia M, Knuckley B, Lee YH, Stallcup MR, Sato M, Thompson PR.** Inhibitors and inactivators of protein arginine deiminase 4: functional and structural characterization. *Biochemistry* 45: 11727–11736, 2006.
22. **Maines LW, Fitzpatrick LR, French KJ, Zhuang Y, Xia Z, Keller SN, Upson JJ, Smith CD.** Suppression of ulcerative colitis in mice by orally available inhibitors of sphingosine kinase. *Dig Dis Sci* 53: 997–1012, 2008.
23. **Makrygiannakis D, af Klint E, Lundberg IE, Lofberg R, Ulfgren AK, Klareskog L, Catrina AI.** Citrullination is an inflammation-dependent process. *Ann Rheum Dis* 65: 1219–1222, 2006.
24. **Mastronardi FG, Wood DD, Mei J, Raijmakers R, Tseveleki V, Dosch HM, Probert L, Casaccia-Bonnefil P, Moscarello MA.** Increased citrullination of histone H3 in multiple sclerosis brain and animal models of demyelination: a role for tumor necrosis factor-induced peptidylarginine deiminase 4 translocation. *J Neurosci* 26: 11387–11396, 2006.
25. **Moscarello MA, Mastronardi FG, Wood DD.** The role of citrullinated proteins suggests a novel mechanism in the pathogenesis of multiple sclerosis. *Neurochem Res* 32: 251–256, 2007.
26. **Moscarello MA, Pritzker L, Mastronardi FG, Wood DD.** Peptidylarginine deiminase: a candidate factor in demyelinating disease. *J Neurochem* 81: 335–343, 2002.
27. **Neuman MG.** Immune dysfunction in inflammatory bowel disease. *Transl Res* 149: 173–186, 2007.
28. **Nikfar S, Rahimi R, Rezaie A, Abdollahi M.** A meta-analysis of the efficacy of sulfasalazine in comparison with 5-aminosalicylates in the induction of improvement and maintenance of remission in patients with ulcerative colitis. *Dig Dis Sci* 54: 1157–1170, 2009.

29. **Reagan-Shaw S, Nihal M, Ahmad N.** Dose translation from animal to human studies revisited. *FASEB J* 17: 659–661, 2007.
30. **Sartor RB.** Mechanisms of disease: pathogenesis of Crohn's disease and ulcerative colitis. *Nat Clin Pract Gastroenterol Hepatol* 3: 390–407, 2006.
31. **Satoh K, Kawakami A, Shirabe S, Tamai M, Sato A, Tsujihata M, Nagasato K, Eguchi K.** Anti-cyclic citrullinated peptide antibody (anti-CCP antibody) is present in the sera of patients with dementia of Alzheimer's type in Asian. *Acta Neurol Scand* 30: 338–341, 2009.
32. **Shepela C.** The safety of biologic agents in the treatment of inflammatory bowel disease. *Minn Med* 91: 42–45, 2008.
33. **Siegel CA, Marden SM, Persing SM, Larson RJ, Sands BE.** Risk of lymphoma associated with combination anti-tumor necrosis factor and immunomodulator therapy for the treatment of Crohn's disease: a meta-analysis. *Clin Gastroenterol Hepatol* 7: 874–881, 2009.
34. **Skopek TR, Liber HL, Penman BW, Thilly WG.** Isolation of a human lymphoblastoid line heterozygous at the thymidine kinase locus: possibility for a rapid human cell mutation assay. *Biochem Biophys Res Commun* 84: 411–416, 1978.
35. **Snider AJ, Kawamori T, Bradshaw SG, Orr KA, Gilkeson GS, Hannun YA, Obeid LM.** A role for sphingosine kinase 1 in dextran sulfate sodium-induced colitis. *FASEB J* 23: 143–152, 2009.
36. **Struyf S, Noppen S, Loos T, Mortier A, Gouwy M, Verbeke H, Huskens D, Luangsay S, Parmentier M, Geboes K, Schols D, Van Damme J, Proost P.** Citrullination of CXCL12 differentially reduces CXCR4 and CXCR7 binding with loss of inflammatory and anti-HIV-1 activity via CXCR4. *J Immunol* 182: 666–674, 2009.
37. **Szodoray P, Szabo Z, Kapitany A, Gyetvai A, Lakos G, Szanto S, Szucs G, Szekanecz Z.** Anti-citrullinated protein/peptide autoantibodies in association with genetic and environmental factors as indicators of disease outcome in rheumatoid arthritis. *Autoimmun Rev* 7: 140–143, 2009.
38. **van Schaardenburg D, Dijkmans BA.** Clinical approaches to early inflammatory arthritis. *Nat Rev Rheumatol* 5: 627–633, 2009.
39. **Whiting PF, Smidt N, Sterne JA, Harbord R, Burton A, Burke M, Beynon R, Ben-Shlomo Y, Axford J, Dieppe P.** Systematic review: accuracy of anti-citrullinated peptide antibodies for diagnosing rheumatoid arthritis. *Ann Intern Med* 152: W155–W466, 2010.
40. **Yamada R, Suzuki A, Chang X, Yamamoto K.** Peptidylarginine deiminase type 4: identification of a rheumatoid arthritis-susceptible gene. *Trends Mol Med* 9: 503–508, 2003.
41. **Ying L, Hofseth AB, Browning DD, Nagarkatti M, Nagarkatti PS, Hofseth LJ.** Nitric oxide inactivates the retinoblastoma pathway in chronic inflammation. *Cancer Res* 67: 9286–9293, 2007.